



Trapping the HIV-1 V3 loop in a helical conformation enables broad neutralization

In the format provided by the authors and unedited

Supplementary information

Trapping the HIV-1 V3 Loop in a Helical Conformation Enables Broad Neutralization

Matthias Glögl¹, Nikolas Friedrich^{1§}, Gabriele Cerutti^{2§}, Thomas Lemmin^{1§}, Young D. Kwon^{3§}, Jason Gorman³, Liridona Maliqi¹, Peer R. E. Mittl⁴, Maria C. Hesselman¹, Daniel Schmidt¹, Jacqueline Weber¹, Caio Foulkes¹, Adam S. Dingens⁵, Tatsiana Bylund³, Adam S. Olia³, Raffaello Verardi³, Thomas Reinberg⁴, Nicolas S. Baumann¹, Peter Rusert¹, Birgit Dreier⁴, Lawrence Shapiro^{2,6}, Peter D. Kwong³, Andreas Plückthun⁴, Alexandra Trkola^{1*}

1 Institute for Medical Virology, University of Zurich (UZH), Zurich, Switzerland.

2 Zuckerman Mind Brain Behavior Institute, Columbia University, New York, NY, USA

3 Vaccine Research Center, National Institute of Allergy and Infectious Diseases, National Institutes of Health, Bethesda, MD, USA.

4 Department of Biochemistry, University of Zurich (UZH), Zurich, Switzerland.

5 Fred Hutchinson Cancer Research Center, Seattle, WA, USA

6 Department of Biochemistry and Molecular Biophysics, Columbia University, New York, NY, USA

§ contributed equally

* correspondence: trkola.alexandra@virology.uzh.ch

Content

1) Supplementary note: DARPIn N-cap displacement	2
2) Supplementary Discussion	4
3) Supplementary Tables	7
Table S1: Virus panels.....	7
Table S2: Neutralization breadth and potency of V3 directed DARPins and antibodies	8
Table S3: Neutralization of JRCSF variants.....	10
Table S4: Inhibitor Source	11
4) Supplementary Figures	12
S1: Flow cytometry and gating strategy	12
S2: Sequence entropy in V3 and the CD4 binding site.....	13
S3: V4-CD4i bnDs are differentially influenced by N-cap framework mutations or removal	14
S4: Conservation of V3	15
4) References.....	16

1) Supplementary note: DARPin N-cap displacement

Structural analysis of bnD.8 and bnD.9 (Fig. 4) pointed towards a (partial) unfolding of the N-cap or a displacement with N-cap residue D28 acting as a hinge. This displacement appears to be required for bnD.9 accessing the V3-stem at this angle in the open trimer structure due to space constraints (Fig. 4D), and it leads to an additional interface with the gp120 bridging sheet. A hydrogen bond forms between DARPin H49 and Env K420 in the gp120 bridging sheet. Of note, residue H49 is positioned in the inner domain of the DARPin (Extended Data Fig. 4B) and is not available for interaction when the cap is not displaced. We therefore investigated the N-cap displacement observed with bnD.9 further, as it may provide insights into the general accessibility of α V3C. Framework regions of N- and C-caps are conserved in the DARPin library design to maintain the functionality of the DARPin scaffold — mutations in these regions are therefore rare. We detected an unusual D15L mutation in the N-cap of bnD.9 that results in rearrangement by pushing R19 and subsequent loss of two N-cap-stabilizing salt bridges made by R19 (Supplementary Fig. 3a). Notably, we observed unusual mutations in the interface of N-cap and first internal ankyrin repeat in 5 of 8 V3-CD4i bnDs but not in any of the V3-crown bnDs (Extended Data Fig. 2). This strongly hints at a feature selected during the ribosome display selection, which allows mutagenesis to happen during PCR. The remaining V3-CD4i bnDs, including bnD.8, had the original scaffold sequence, suggesting that they may not require an N-cap shift to bind. To investigate this further, we performed docking analyses with bnD.8 using a series of frames derived from the MD simulations, showing that bnD.8 can successfully approach the target by a change in the angle of the protruding α V3C (Extended Data Fig. 7D). To explore the importance of the N-cap for binding and neutralization and the influences of potentially destabilizing mutations, we generated constructs without N-cap, and with non-mutated (D15, as in bnD.8) or mutated (D15L, as in bnD.9) N-cap. Removal of the N-cap increased the potency for bnD.9 substantially (11.8-fold, Supplementary Fig. 3B). Interestingly, restoring the N-cap also increased the potency of bnD.9 to a similar degree, and the median potency of bnD.8 without N-cap was only moderately better compared to bnD.8 (3.8-fold). Taken together, this indicates that the efficacy of bnDs with or without a mutated N-cap was similar overall. Conversely, however, mutation of the bnD.8 N-cap reduced potency. This pattern is consistent with a scenario in which binding for both DARPins is initiated with the N-cap in place, and N-cap displacement occurs secondary to this.

Although N-cap displacement does not appear to be required for neutralization, the truncation of both bnD.9 and bnD.8 likely benefits the interaction with the trimer by reducing overall steric hindrance and introducing an additional hydrophobic interface with the gp120 bridging. Thus we explored the potential for enhancing the bridging-sheet interactions by performing an in-silico optimization of bnD.9 with Rosetta^{1,2} (Figure S8C). Mutations suggested to augment the binding energy (L43I, F47E, and I52M) indeed resulted in an increase in potency and breadth of truncated bnD.9 (Supplementary Fig.

3D; Extended Data Fig. 3). Within the 42-virus panel examined, only three strains were resistant (ZEnv32_0111_5, ZEnv16_1202_7, and Q769_h5), the latter two of which carry a deletion in V3 that is expected to twist the helix interface, further highlighting the importance of the α V3C helix for engagement by V3-CD4i bnDs.

To further investigate accessibility of α V3C for antibody-like molecules in vitro, we generated C-terminal Fc-fusion proteins composed of the most potent versions of bnD.8 and bnD.9, respectively, and the constant region of human IgG1. Although a substantial loss in neutralization capacity against Tier-2 viruses was evident, some neutralization was retained, and constructs stayed active against Tier-1 strain Bal26 and enhanced activity against SF162 (Extended Data Fig. 8B). Upon binding α V3C, the bnD C-terminus is expected to be close to the host cell membrane. We therefore considered that fusion of the Fc to the C-terminus may have added further access constraints. We therefore investigated an alternate antibody-like bnD complex in which the bnD is connected N-terminally to the antibody part. To achieve this, we complexed N-terminally his-tagged bnD with an anti-his-tag antibody. Although this antibody-bnD complex is larger than the bnD-Fc fusion proteins, we observed a higher neutralization capacity towards Tier-2 viruses (Extended Data Fig. 8B). Collectively, these data support the notion that access for α V3C antibodies is possible. In the context of MPER bnAbs, IgG3 molecules were considered advantageous for accessing the MPER region near the viral lipid membrane due to their extended and more flexible hinge region^{3,4}. Interestingly, our model also suggests that α V3C, which is located close to the cell membrane in the CD4-bound state, would also be more accessible to IgG3 molecules.

2) Supplementary Discussion

In this study, we defined an intermediate conformational state of the V3 loop that serves as target for broad neutralization. High-resolution structural analysis of flexible proteins and subdomains such as the V3 loop on HIV-1 Env requires fixation, usually by high-affinity ligands. Therefore, to obtain information on native conformations, the selected ligands should ideally capture the protein without forcing an induced fit upon binding. Using the DARPIn technology, we have developed a strategy to localize and resolve V3 conformations associated with broad neutralization capabilities. Due to their rigid binding surface, DARPins are often highly dependent on the conformation of the target, and, as we show here, can be used to define novel HIV-1 Env substructures that have eluded conventional structural analysis of antibody-ligated complexes.

To prove the concept that V3 is amenable to broad neutralization beyond the established V3-glycan bnAb epitopes, we generated a range of broadly neutralizing DARPIn (bnD) inhibitors targeting V3 in an open CD4-induced Env state. The selected bnDs matched the breadth of the V3-glycan bnAbs (60-79%) but showed lower potency, which is likely due to their mode of action post CD4 binding⁵. Indeed, all post-CD4 attachment inhibitors, including antibodies that act after CD4 binding like MPER bnAbs, show lower potency compared with pre-attachment inhibitors⁶⁻¹¹.

Using the novel V3-CD4i bnDs to define the target site for broad neutralization, we show that the V3 adopts a previously unrecognized conformation, a 4-turn alpha helix that we term α V3C. We postulate that this conformation is also sampled without ligand binding during the entry process, based on several lines of evidence. We observed the α V3C conformation in complex with two unrelated DARPins obtained from independent Ribosome Display selections using different panning targets. Molecular dynamics simulations highlight that the helix is stable in the absence of the DARPIn ligand and is supported by additional salt bridges between conserved residues that are not functionally required for co-receptor interaction. Considering the strong immune pressure on V3, it would be difficult to comprehend, that such an extended helix-forming stretch is maintained without functional relevance. In the five independent screens that gave rise to α V3C DARPins, a range of Env probes were included comprising open and closed Env conformations that all at least partially expose the V3 region. Whether a fraction of the panning proteins spontaneously sampled the α V3C conformation or whether binding to unstructured V3 sufficed for selection, cannot be deferred from these experiments but irrespective of this, these parallel selections underline that α V3C targeting molecules are not a chance finding and the appropriate target regions were sufficiently exposed. It is conceivable that the amphipathic α V3C helix interacts with the host membrane during coreceptor interaction through its hydrophobic face. Indeed, helix-breaking amino acids within the α V3C stretch are rare in circulating strains

(Supplementary Fig. 4), are not well tolerated *in vitro* in the absence of an immune response¹² and were not enriched in escape to V3-CD4i bnDs (Fig. 5B). Two strains, Q769_h5 and ZEnv16_1202_7, that remained resistant to optimized bnD.9 indeed have deletions in V3 (Extended Data Fig. 3). These deletions are in principle compatible with helix formation but would be expected to twist the helix interface away of the DARPIn and thereby blocking access. A propensity of V3 to form amphipathic helices has been reported in NMR studies with helices stretching from residues 320-328¹³ and 324-330¹⁴ and in complex with CCR5¹⁵, the V3-crown DARPIn bnD.2⁵ and the vaccine-induced rabbit antibody 10A37¹⁶. While these previously described V3 helices are considerably shorter than α V3C, they highlight the domain's conserved predisposition to adopt an α -helical structure. Taken together, these lines of evidence suggest a functional significance of the α V3C helix that warrants further investigation to decipher its sensitivity to broad neutralization. Most notably, the similarities of the N-terminal helix turns of α V3C to the described CCR5-bound V3 conformation are striking and suggest a possible involvement of the α V3C region in accessing the co-receptor pocket. Neutralizing antibodies targeting the V3 C-terminal half have not been described in HIV-1 infection. The V3 response is dominated by non-neutralizing N-terminal half and GPG-specific antibodies¹⁷⁻²⁰. These antibodies will strongly compete with C-terminal half Abs that bind to α V3C. Although the α V3C region likely requires CD4 triggering for formation and is presumably transiently exposed during entry, our data indicate that antibody access to α V3C is possible (Extended Data Fig. 8). Therefore, further investigation of whether α V3C-directed antibodies develop *in vivo* or can be induced by vaccination is highly warranted. This may provide opportunities to create α V3C scaffold immunogens to elicit novel bnAbs that match the properties of V3-CD4i bnDs. Moreover, even though we observe binding mostly on open Env and post-attachment, spontaneous opening of Env and thus also sampling of α V3C pre-attachment may occur²¹⁻²³.

The relatively low potency paired with high breadth of α V3C directed bnDs is in line with their limited opportunity for access, and is reminiscent to what has been observed for post-attachment neutralization active antibodies²⁴. However, if considered for *in vivo* application, the present bnDs may be engineered to high potency taking advantage of the versatile DARPIn system, by improving affinity and gaining avidity through multimerization²⁵.

We hypothesize that α V3C directed antibodies, should they indeed evolve *in vivo* or be inducible by vaccination, will share the features of post-attachment bnAbs and bnDs and be broad but not potent. Given that this type of inhibitor provides an additional layer of viral control by targeting the cell-bound virion, its activity should nevertheless be exploited for prevention, as it may provide another piece of the puzzle on the path to sterilizing immunity through an HIV vaccine.

Collectively, the definition of the α V3C helix illustrates the high conformational diversity of the Env trimer, where flexible subdomains adopt different conformations within the main open and closed states, providing conserved surfaces for recognition.

3) Supplementary Tables

Table S1: Virus panels

Subtype	Tier	Virus	5-virus panel	13-virus panel	42-virus panel	Genbank entry code
AE	2	ZEnv32_0111_5			x	KU600816
B	2	RHPA4259 clone 7		x	x	AY835447
B	2	ZEnv16_1202_7			x	KU600818
G	2	NAB13pre_cl_9			x	EU023937
B	1B	BaL_26			x	DQ318211
B	2	QH0692 clone 42			x	AY835439
A	2	MG505_WOM_ENV_A2 A1			x	DQ208449
G	2	X2088		x	x	EU885764
B	2	REJO4541 clone 67		x	x	AY835449
A	2	Q769_h5		x	x	AF407159
AE	2	C1080_c03	x	x	x	JN944660
B	2	ZEnv07_0504_15			x	KU600814
B	2	NAB5pre_cl_1			x	EU023923
AG	2	CRF02_cl_250			x	EU513189
C	2	HIV-001428-2			x	EF117266
B	2	TRO clone 11			x	AY835445
C	2	DU422		x	x	AY043175
B	2	JR-CSF			x	AY669726
C	1B	HIV_25925_2			x	EF117273
C	2	ZM106F.PB9			x	AY424163
C	2	53M12		x	x	AY423984
B	3	PVO clone 4			x	AY835444
A	2	KER2018.11			x	AY736810
C	2	ZM214M.PL15			x	DQ3885
BC	1B	CNE40			x	HM215414
B	2	ZEnv91_0505_12			x	KU600815
AE	2	CNE5			x	HM215415
G	2	CRF02_cl_252			x	EU513190
C	2	ZM249M.PL1			x	DQ388514
A1D	unclassified	0815_v3_c3		x	x	HM215260
B	2	NAB9pre_cl_106			x	EU023928
C	2	CAP88.6m.c10			x	KU198436
B	2	JR-FL	x	x	x	AY669728
C	2	ZM233M.PB6		x	x	DQ388517
C	2	CAP45_2_00_G3	x	x	x	DQ435682
AE	2	ZEnv92_1008_8			x	KU600817
A	2	Q842_d12_PNS70d A1		x	x	AF407160
C	2	Du156.12			x	DQ411852
A	2	BG505_W6M_ENV_A5_T332N	x	x	x	DQ208456
B	2	WITO4160 clone 33	x		x	AY835451
AE	2	CNE59			x	HM215422
A	1B	Q23_17			x	AF004885

Table S1: Virus panels

Table S2: Neutralization breadth and potency of V3 directed DARPins and antibodies IC₅₀ summary of DARPins and mAb activity against the 42-virus multi-clade panel (Figure 1). Maximum concentrations of inhibitors probed were 10'000 nM for DARPins and 167 nM (25 µg/mL) for antibodies. If no inhibition >50% was obtained at the highest concentration tested, this is listed as ">10'000 nM" or ">167 nM", respectively. Data are derived from one to three independent experiments. nd: not determined

Table S3: Neutralization of JRCSF variants

	Antibodies ($\mu\text{g/mL}$)			DARPinS (μM)				
	17b	447-52D	PGT128	bnD.2	bnD.3	bnD.4	bnD.8	bnD.9
JRCSF WT	2.987	12.570	0.0077	0.4520	0.2254	0.6422	0.0722	2.8990
L125A	0.006	0.006	0.0165	0.1039	0.0254	0.0159	0.0018	0.0313
N156A	0.029	0.006	0.0115	0.0456	0.0161	0.0285	0.0005	0.0818
Y177A	0.019	0.006	0.0222	0.0212	0.0122	0.0160	0.0001	0.0127
N197K	0.129	0.005	0.0153	0.1067	0.0559	0.0725	0.0012	0.2066
S199A	2.630	0.010	0.0221	0.1701	0.0596	0.1167	0.0083	0.4807
T202A	0.069	0.006	0.0109	0.0701	0.0632	0.0550	0.0119	0.2926
N301A	0.169	0.006	0.0961	0.1279	0.0299	0.0274	0.0021	0.1343
T303A	0.088	0.006	0.1072	0.0474	0.0234	0.0278	0.0027	0.2525
K305A	0.018	0.006	0.0140	0.0663	0.0416	0.0321	0.0046	0.0808
I307A	0.067	0.006	0.0889	0.0437	0.0030	0.0113	0.0007	0.0555
I309A	0.029	0.006	0.0104	1.8989	0.2557	0.0289	0.0006	0.0882
Y318A	0.134	0.006	0.0108	5.1047	3.1577	3.5240	0.0046	0.1604
I323A	0.019	0.006	0.0124	0.0395	0.0275	0.0276	0.0031	0.1756
G324A	0.081	0.006	0.0238	0.0266	0.0265	0.0182	0.0025	0.0758
I420A	21.795	0.006	0.0171	0.5511	0.1390	0.6092	0.0197	0.4383
K421A	0.220	0.006	0.0121	0.3461	0.0329	0.0905	0.0008	0.4289
I423A	1.096	0.006	0.0285	0.0653	0.0494	0.0108	0.1871	0.5721
I424A	4.239	0.006	0.0107	0.2196	0.0863	0.3379	0.0169	0.4613
Y435A	6.251	0.006	0.0065	0.1926	0.1539	0.2663	0.0144	0.6848

Table S3: Neutralization of JRCSF variants Neutralization potency of bnD.8, bnD.9 and antibodies against a panel of alanine mutants in JRCSF Env. Maximum concentrations of inhibitors probed were 10,000 nM for DARPinS and 167 nM (25 $\mu\text{g/mL}$) for antibodies. IC50 values shown are means from two to three independent experiments.

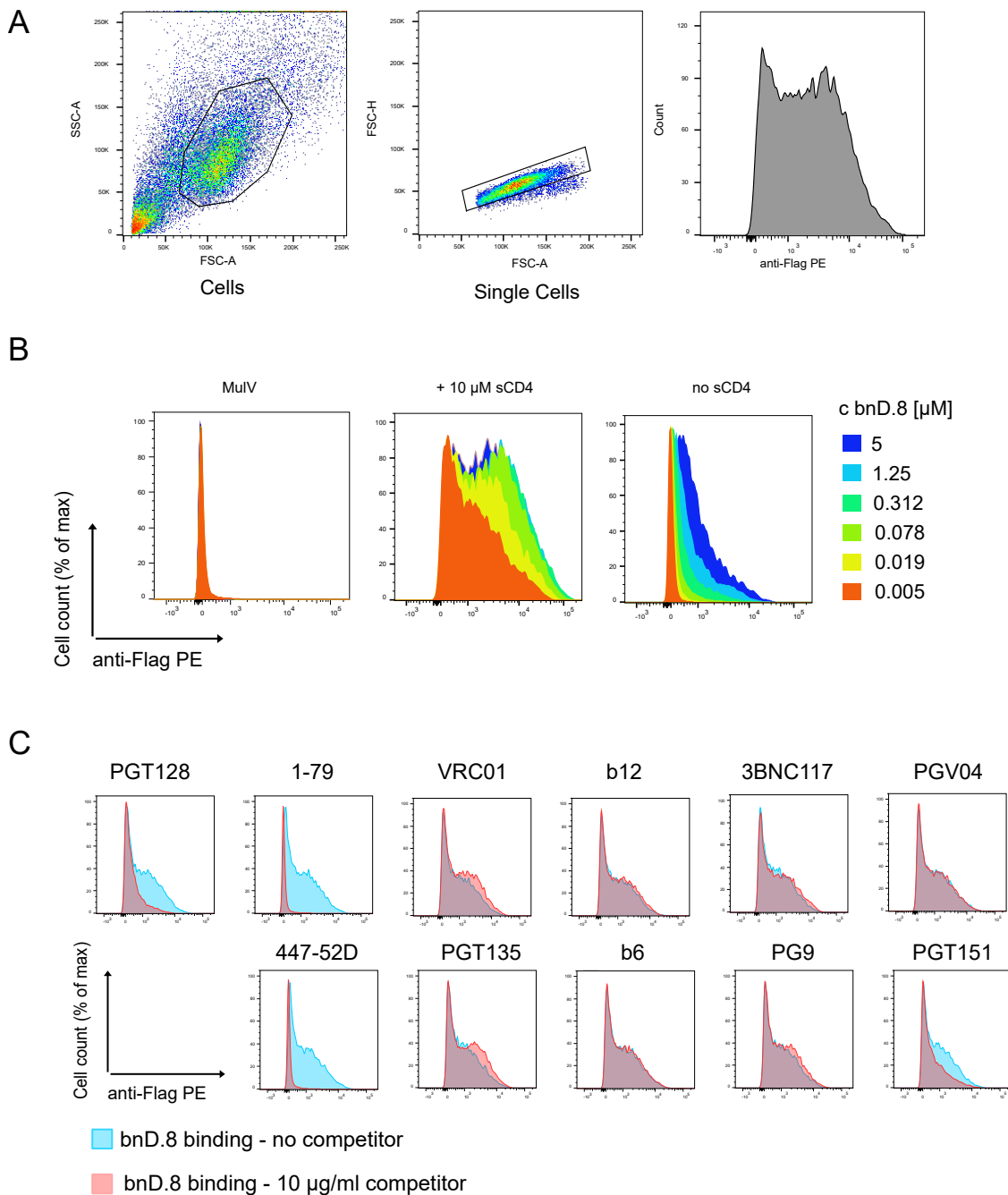
Table S4: Inhibitor Source

Name	Epitope	Reference	Source
b12	CD4bs	Barbas III et al. 1992 PNAS. 89(19):9339-43	D. Burton, The Scripps Research Institute, La Jolla, USA
b6	CD4bs	Barbas III et al. 1992 PNAS. 89(19):9339-43	D. Burton, The Scripps Research Institute, La Jolla, USA
3BNC117	CD4bs	Scheid et al. 2011 Science 16;333(6049):1633-7	M. Nussenzweig, The Rockefeller University, New York, USA
PGV04	CD4bs	Wu et al. 2010 Science. 329(5993):856-61	J. Mascola*, Vaccine Research Center, National Institutes of Health, Bethesda, USA
VRC01	CD4bs	Wu et al. 2010 Science. 329(5993):856-61	J. Mascola*, Vaccine Research Center, National Institutes of Health, Bethesda, USA
NIH45-46	CD4bs	Scheid et al. 2011 Science 16;333(6049):1633-7	M. Nussenzweig, The Rockefeller University, New York, USA
CD4-IgG2	Cd4bs	Allaway et al. 1995 AIDS Res Hum Retroviruses	W. Olson*, Progenics Pharmaceuticals Inc
17b	CD4i	Thali et al. 1993 J Virol. 67(7):3978-88	J. Robinson, Tulane University Medical Center, New Orleans, USA
48d	CD4i	Thali et al. 1993 J Virol. 67(7):3978-88	J. Robinson, Tulane University Medical Center, New Orleans, USA
2G12	High Mannose Patch	Trkola et al. 1996 J Virol. 70(2):1100-8	H. Katinger and D. Katinger, Polymun, Vienna, Austria
8ANC195	Interface/Fusionpeptide	Scharf et al. 2014 Cell Rep. 7(3): 785-795.	Own production
35O22	Interface/Fusionpeptide	Huang et al. 2014 Nature. 515(7525):138-42	J. Mascola*, Vaccine Research Center, National Institutes of Health, Bethesda, USA
PGT151	Interface/Fusionpeptide	Falkowska et al. 2014 Immunity 40(5): 657-668.	Own production
10E8	MPER	Huang et al. 2012 Nature. 491(7424):406-12	12 M. Connors*, National Institute of Allergy and Infectious Diseases, NIH, Bethesda, USA
4E10	MPER	Stiegler et al. 2001 AIDS Res Hum Retroviruses. 17(18):1757-65	H. Katinger and D. Katinger, Polymun, Vienna, Austria
2F5	MPER	Buchacher et al. 1994 AIDS Res Hum Retroviruses. 10(4):359-69	H. Katinger and D. Katinger, Polymun, Vienna, Austria
VRC26.09	V2 Glycan	Doria-Rose et al., 2014 Nature 509, 55-62	L.Morris, P. Moore, National Institute for Communicable Diseases, South Africa
VRC26.25	V2 Glycan	Doria-Rose et al., 2014 Nature 509, 55-62	L.Morris, P. Moore, National Institute for Communicable Diseases, South Africa
PGT145	V2 Glycan	Walker et al. 2011 Nature. 477(7365):466-70	D. Burton, The Scripps Research Institute, La Jolla, USA
PG16	V2 Glycan	Walker et al. 2009 Science. 326(5950):285-9	D. Burton, The Scripps Research Institute, La Jolla, USA
PG9	V2 Glycan	Walker et al. 2009 Science. 326(5950):285-9	D. Burton, The Scripps Research Institute, La Jolla, USA
PGT135	V3 High Mannose Patch	Walker et al. 2011 Nature. 477(7365):466-70	D. Burton, The Scripps Research Institute, La Jolla, USA
PGT128	V3 High Mannose Patch	Walker et al. 2011 Nature. 477(7365):466-70	D. Burton, The Scripps Research Institute, La Jolla, USA
10-1074	V3 High Mannose Patch	Mouquet et al. PNAS 2012 109 (47) 19059-19060;	M. Nussenzweig, The Rockefeller University, New York, USA
PGT121	V3 High Mannose Patch	Walker et al. 2011 Nature. 477(7365):466-70	D. Burton, The Scripps Research Institute, La Jolla, USA
447-52D	V3-Crown	Gorny et al. 1992 J Virol. 66(12):7538-42	H. Katinger and D. Katinger, Polymun, Vienna, Austria
1-79	V3-Crown	Scheid et al. 2009 Nature. 458(7238):636-40	M. Nussenzweig, The Rockefeller University, New York, USA

* Through the NIH AIDS Reagent Program, Division of AIDS, NIAID, NIH

4) Supplementary Figures

S1: Flow cytometry and gating strategy



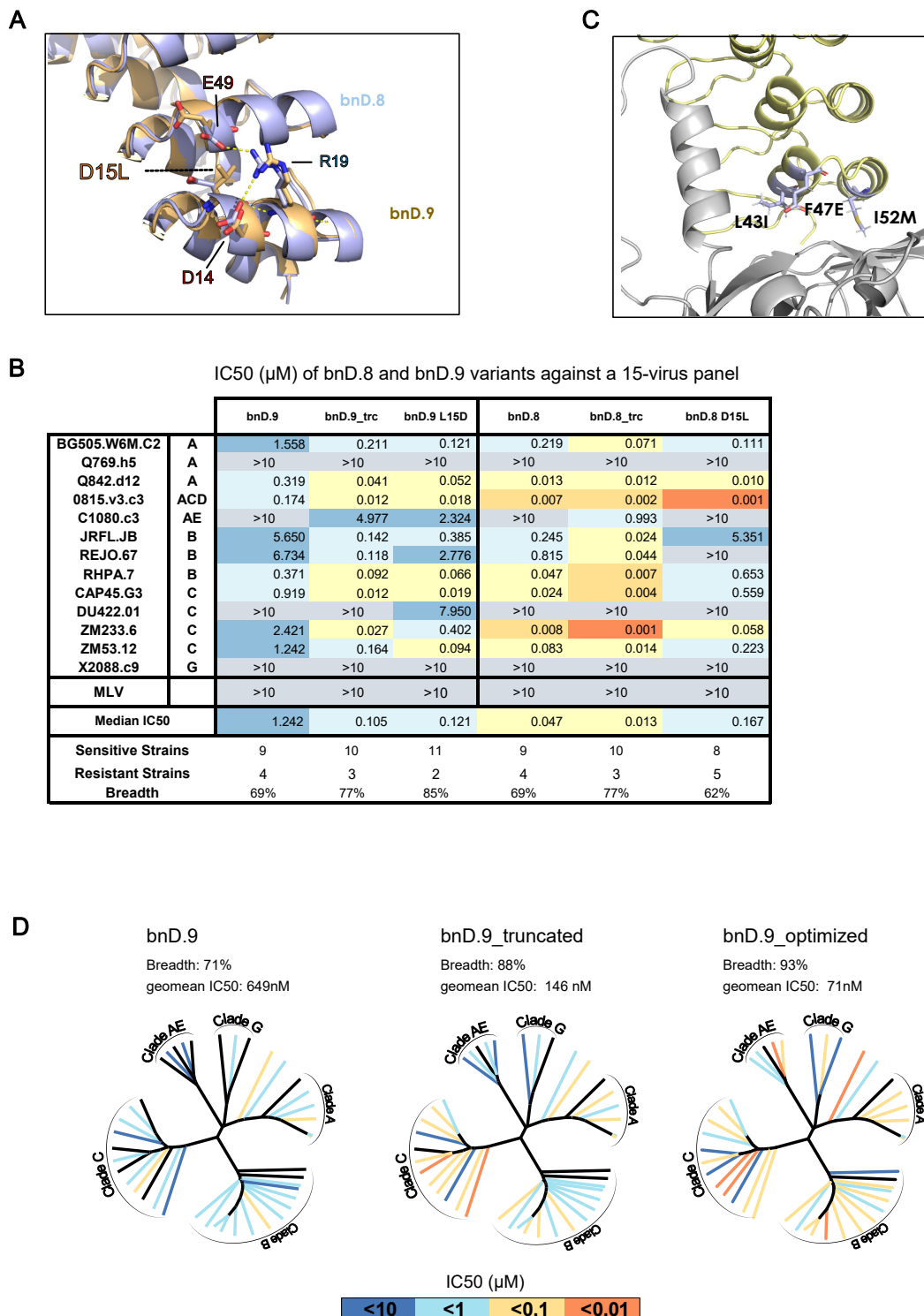
Supplementary Fig. 1. Flow cytometry and gating strategy **A)** Gating strategy to obtain single cells from the pool of HEK 293 T cells harvested 36h post-transfection with Env-expression plasmid. **B)** bnD.8 binding to SF162 in the presence or absence of 10 μ M sCD4. Mulv Env served as negative control. Histograms of normalized fluorescence intensities are shown. Related to Fig. 2C **C)** Binding of 10 μ M bnD.8 in the presence or absence of 10 μ g/ml competitor antibodies. Histograms of normalized fluorescence intensities are shown. Related to Fig. 2F

S2: Sequence entropy in V3 and the CD4 binding site

V3 residue	Sequence entropy based on 42 virus panel	Sequence entropy based on M env strains	X5	CCR5	17b	bnD.9	10A35	bnD.2	bnD.3	447-52D	268-D
296	0.04	0.01									
297	0.39	0.37									
298	0.04	0.01									
299	0.16	0.09									
300	0.46	0.54									
301	0.09	0.1									
302	0.04	0.1									
303	0.09	0.13									
304	0.09	0.14		x						x	x
305	0.35	0.49		x	x				x	x	x
306	0.09	0.32		x	x				x	x	x
307	0.21	0.39		x	x			x	x	x	x
308	0.62	0.72		x	x		x	x	x	x	x
309	0.21	0.36		x	x	x	x	x	x	x	x
312	0.09	0.08		x		x	x	x	x	x	x
313	0	0.14		x		x	x	x	x	x	x
314	0.04	0.04		x		x	x	x	x	x	x
315	0.34	0.52		x		x	x	x	x	x	x
316	0.42	0.53	x	x		x		x	x		
317	0.13	0.33		x		x	x	x	x	x	x
318	0.12	0.23		x		x	x	x	x	x	
319	0.37	0.44		x	x		x	x			
320	0.09	0.3		x	x		x	x	x		
321	0.24	0.4				x	x				
321a	0.52	0.74		x			x				
322	0.04	0.17		x		x	x				
323	0.15	0.26		x	x		x				
324	0	0.05		x		x					
325	0.31	0.28		x							
326	0.09	0.1		x	x	x	x				
327	0.04	0.05		x	x		x				
328	0.37	0.47				x					
329	0.04	0.02									
330	0.25	0.35									
331	0	0.01									

CD4bsresidue	Sequence entropy based on 42 virus panel	Sequence entropy based on M env
102	0.36	0.34
124	0.04	0.05
125	0.04	0.06
126	0.04	0.01
127	0.04	0.04
128	0.04	0.12
194	0.16	0.24
196	0	0.02
257	0.04	0.01
279	0.3	0.4
280	0.09	0.08
281	0.46	0.5
283	0.41	0.45
364	0.27	0.28
365	0	0.02
366	0.04	0.01
367	0.04	0.01
369	0.04	0.02
370	0.26	0.23
424	0.15	0.18
425	0.16	0.31
426	0	0.03
427	0.04	0.06
428	0.44	0.62
429	0.19	0.2
430	0.04	0.05
431	0.47	0.52
454	0.26	0.32
455	0.09	0.12
456	0.04	0.04
457	0.04	0.08
458	0.13	0.17
459	0.88	0.62
460	0.75	0.87
468	0	0.04
470	0.19	0.43
471	0.04	0.02
472	0.04	0.02
473	0.3	0.32
475	0.31	0.32

Supplementary Fig. 2: Sequence entropy in V3 and the CD4 binding site **A)** Sequence entropy of V3 residues based on the 42-virus panel (Table S1) and all 7590 group M strains listed in the NIH sequence database as of May 2021 are shown. Residues that are recognized by an antibody/DARPin/CCR5 (with non-zero buried surface area) are marked as “x” in the corresponding column. **B)** Sequence entropy of CD4bs epitope residues based on the 42-virus panel and group M strains are shown.

S3: V4-CD4i bnDs are differentially influenced by N-cap framework mutations or removal**Supplementary Fig. 3: V4-CD4i bnDs are differentially influenced by N-cap framework mutations or removal**

A) Rearrangement of interactions between the first (N-cap) and second ankyrin repeat observed as a consequence of the bnD.9 backbone mutation D15L. Comparison between bnD.8 (light blue) and bnD.9 (gold) depicts loss of salt bridges to Arg19 by the D15L mutation in bnD.9 **B)** Neutralization capacity of bnD.9 and bnD.8 N-cap variants. Variants of bnD.8 and bnD.9 with the N-cap deleted (bnD.8_trc and bnD.9_trc) as well as bnD.9 L15D and bnD.8 D15L versions were compared to the parental constructs. Median IC50s were calculated over all sensitive strains. **C)** Location of interface mutations introduced into bnD.9_trc to optimize binding to gp120 as defined by Rosetta. Changed residues are shown as sticks and labels indicating the mutation. **D)** Comparison of neutralization capacity of bnD.9 variants on the 42-virus panel. IC50 values of three bnD.9 variants are indicated for 42 virus strains by color code on the phylogenetic trees.

S4: Conservation of V3

HXB2		A	C	D	E	F	G	H	I	K	L	M	N	P	Q	R	S	T	V	W	Y	gap						
296	C	0	99.88	0	0	0.02	0	0	0	0	0	0	0	0	0.04	0	0	0	0	0.06	0	99.9	C	0.06	Y	0.04	R	
297	T	1.19	0	0	0.68	0.02	0	0.02	12.2	0.08	0.2	1.02	0	0	0.06	0.06	1.83	79.8	2.83	0	0.04	0	79.8	T	12.17	I	2.83	V
298	R	0	0	0	0	0	0.08	0	0	0.12	0	0	0	0	0	99.8	0	0.02	0	0	0	99.8	R	0.12	K	0.08	G	
299	P	0.06	0	0	0	0.1	0	0.42	0.06	0	0.94	0	0.1	98	0	0	0	0.5	0.24	0	0.04	0	97.6	P	0.94	L	0.5	T
	-	0	0	0	0	0.02	0.02	0	0	0	0	0	0.1	0	0	0	0	0	0	0	0.02	100	0.06	N	0.02		0.02	
300	N	0.6	0.02	0.54	0	1.31	16.6	1.14	0.06	0.02	0	0	60	0	0.16	0.04	16.4	0.28	0	0	2.47	0	60.4	N	16.55	G	16.37	S
301	N	0	0	0.42	0.3	0	0.04	0.12	0.22	0.82	0	0.02	97	0	0.08	0.22	0.3	0.56	0.08	0	0.14	0.1	96.6	N	0.82	K	0.56	T
302	N	0.02	0.02	0.04	0	0	0.06	0.22	0.2	1.1	0	0	97	0	0	0.18	0.32	0.44	0.04	0	0.46	0	96.9	N	1.1	K	0.46	Y
303	T	0.06	0	0	0.08	0	0.02	0	1.85	1.08	0.06	0.16	0	0	0.14	0.76	0.16	95.1	0.54	0	0	0	95.1	T	1.85	I	1.08	K
304	R	0.08	0	0	0.08	0.02	0.16	0	1.33	0.9	0.24	0.14	0	0	0.12	95.3	1.29	0.14	0.12	0	0	0	95.3	R	1.33	I	1.29	S
305	K	0.08	0	0.04	1.71	0	0.14	0.04	0.48	67.2	0.04	0.08	0.3	0	4.06	12.6	0.14	12.9	0.16	0	0.02	0	67.2	K	12.94	T	12.6	R
306	R	0.06	0	0.24	0.06	0.02	14.3	0.04	0.18	0.32	0	0.02	0.2	0.1	0.14	4.04	80	0.14	0.04	0.02	0.06	0	80	S	14.34	G	4.04	R
	-	0	0	0	0	0	0.04	0.04	0.2	0.02	0	0	0	0	0.22	0.12	0.02	0.02	0	0	0	99	0.22	R	0.2	I	0.12	S
307	I	0.18	0	0	0.1	0.28	0	0.16	71.6	0.04	0.88	3.86	0	0	0	0.08	0.1	3.11	19.4	0.08	0.1	0	71.6	I	19.43	V	3.86	M
308	R	0.54	0	0.02	0	0.02	1.99	31.4	0.12	0.06	0.06	0.04	4.7	6.7	1.15	41.6	4.48	6.59	0.08	0.06	0.48	0	41.6	R	31.38	H	6.71	P
309	I	0	0	0	0	2.05	0.14	0	79.2	0.04	7.85	9.28	0	0	0	0.18	0.04	0.34	0.86	0	0.02	0	79.2	I	9.28	M	7.85	L
310	Q	0.02	0	0	0	0	0.58	0.2	0	0	0	0	0	0	0.02	0.06	0	0	0.02	0	0	99	99.1	-	0.58	G	0.2	H
311	R	0.02	0	0	0	0	0.02	0.02	0.52	0	0.02	0	0	0.1	0	0.12	0	0.04	0.04	0	0	99	99.1	-	0.52	I	0.12	R
312	G	2.77	0	0	0.02	0	96.6	0.02	0.04	0	0	0	0	0	0.06	0.12	0.08	0.16	0.18	0	0	0	96.6	G	2.77	A	0.18	V
313	P	0.26	0	0	0	0.28	0.16	0.02	0.1	0.04	0.98	0.02	0	95	1.25	0.42	0.18	0.16	0.12	1.1	0.02	0	94.9	P	1.25	Q	1.1	W
314	G	0.04	0	0	0.04	0	99.5	0	0	0.04	0.06	0.02	0	0	0	0.14	0	0	0	0.06	0	0.1	99.5	G	0.14	R	0.06	W/L
315	R	0.56	0	0	0.06	0.02	1.53	0.86	0.02	5.54	0.1	0	0	0.1	55.6	32.9	2.45	0.06	0.02	0	0.08	0	55.6	Q	32.92	R	5.54	K
316	A	52.25	0	0	0.08	0.12	0.22	0.02	0.5	0.1	0.22	1.02	0	0.2	0.02	0.26	1.95	29.7	13.1	0.08	0.06	0.1	52.3	A	29.69	T	13.12	V
317	F	0.14	0.02	0	0	82	0.02	0	2.97	0	6.35	0.54	0	0	0.04	0.04	0.18	0	0.82	5.36	1.51	0	82	F	6.35	L	5.36	W
318	V	0.1	0	0.16	0	9.6	0	1.67	0.26	0	0.22	0.06	0	0	0.1	0.14	0.24	0.12	0.42	0.4	86.5	0	86.5	Y	9.6	F	1.67	H
319	T	67.36	0.02	0.02	0.04	0.1	0.98	0.08	0.14	1.57	0.14	0.08	0	0.1	0.48	7.61	0.5	18.6	0.56	0	0.64	0.9	67.4	A	18.64	T	7.61	R
320	I	2.45	0	0.04	0.2	0.02	0.7	0.76	0.64	0.34	0.1	0.8	3	0.5	0.24	1.87	1.04	86.7	0.12	0.04	0.4	0.1	86.7	T	3.01	N	2.45	A
321	G	0.42	0	3.74	2.91	0.02	77.9	0.06	0.02	1.81	0.02	0	5.3	0.2	0.4	1.29	0.66	1.04	0	0	0.08	4.1	77.9	G	5.26	N	3.74	D
321a		7.39	0	45	22.1	0	4.94	0.2	0.08	2.11	0	0.04	2	0	5.6	2.07	1.35	0.68	0.12	0	0.06	6.2	45	D	22.06	E	7.39	A
322	K	0.02	0	0	0.02	0	0	0	92.5	0.1	0.12	0.18	0	0	0.04	0.08	0	0.12	6.45	0	0.02	0.3	92.5	I	6.45	V	0.18	M
323	I	0.08	0	0.08	0.18	0.02	0.18	0	86.7	0.54	0.34	0.22	0.1	0	0.08	0.24	0.06	6.69	4.36	0	0.02	0.1	86.7	I	6.69	T	4.36	V
324	G	0.02	0	0.14	0.12	0	99.2	0	0.02	0.1	0	0	0	0	0.02	0.28	0.04	0.06	0	0	0	0	99.2	G	0.28	R	0.14	D
325	N	0.04	0	80	0.82	0	0.12	0.04	0.1	0.78	0	0	17	0.1	0.12	0.06	0.22	0.04	0.02	0	0.12	0.1	80	D	17.36	N	0.82	E
326	M	0.06	0	0.02	0	0	0.04	0	97.4	0.14	0.1	0.16	0	0.7	0	0.1	0.02	0.7	0.38	0	0	0.2	97.4	I	0.72	P	0.7	T
327	R	0.02	0	0	0	0	0.12	0	0.02	1.31	0	0	0	0	0	0	98.3	0.04	0.08	0	0.02	0	98.3	R	1.31	K	0.12	G
328	Q	0.58	0	0.14	3.21	0	0.02	0.32	0.1	20.8	0.64	0.02	0.5	0.1	68.5	4.58	0.36	0.06	0.04	0.02	0.04	0	68.5	Q	20.75	K	4.58	R
329	A	99.56	0	0.02	0	0	0.02	0	0	0	0	0	0	0	0	0	0	0.12	0.14	0.08	0	0	99.6	A	0.14	T	0.12	S
330	H	0.02	0.02	0.02	0.04	1.63	0	70.1	0	0	0.04	0	0.2	0	0.68	0.2	0.62	0	0.02	0.1	26.2	0	70.1	H	26.2	Y	1.63	F
331	C	0	99.78	0.02	0	0.02	0.02	0	0	0	0	0	0	0	0.02	0.06	0.04	0	0	0	0.04	0	99.8	C	99.78	R	0.06	X

Supplementary Fig. 4: Conservation of V3 The amino acid frequency was determined for all positions (HxB2 numbering) in V3 across group M based on 5067 Env sequences not containing premature stop codons or frameshifts downloaded from the Los Alamos National Library HIV-1 Env sequence collection on May 23rd, 2021.

4) References

- 1 Leaver-Fay, A. *et al.* ROSETTA3: an object-oriented software suite for the simulation and design of macromolecules. *Methods Enzymol* **487**, 545-574 (2011). <https://doi.org:10.1016/B978-0-12-381270-4.00019-6>
- 2 Lemay, J. K. *et al.* Macromolecular modeling and design in Rosetta: recent methods and frameworks. *Nature Methods* **17**, 665-680 (2020). <https://doi.org:10.1038/s41592-020-0848-2>
- 3 Rispens, T. *et al.* Dynamics of inter-heavy chain interactions in human immunoglobulin G (IgG) subclasses studied by kinetic Fab arm exchange. *J Biol Chem* **289**, 6098-6109 (2014). <https://doi.org:10.1074/jbc.M113.541813>
- 4 Roux, K. H., Strelets, L. & Michaelsen, T. E. Flexibility of human IgG subclasses. *J Immunol* **159**, 3372-3382 (1997).
- 5 Friedrich, N. *et al.* Distinct conformations of the HIV-1 V3 loop crown are targetable for broad neutralization. *Nature Communications* **12** (2021). <https://doi.org:10.1038/s41467-021-27075-0>
- 6 Reh, L. *et al.* Capacity of Broadly Neutralizing Antibodies to Inhibit HIV-1 Cell-Cell Transmission Is Strain- and Epitope-Dependent. *PLoS pathogens* **11**, e1004966 (2015). <https://doi.org:10.1371/journal.ppat.1004966>
- 7 Gombos, R. B. *et al.* Inhibitory Effect of Individual or Combinations of Broadly Neutralizing Antibodies and Antiviral Reagents against Cell-Free and Cell-to-Cell HIV-1 Transmission. *J Virol* **89**, 7813-7828 (2015). <https://doi.org:10.1128/JVI.00783-15>
- 8 Kim, A. S., Leaman, D. P. & Zwick, M. B. Antibody to gp41 MPER alters functional properties of HIV-1 Env without complete neutralization. *PLoS pathogens* **10**, e1004271 (2014). <https://doi.org:10.1371/journal.ppat.1004271>
- 9 Lai, R. P. *et al.* A fusion intermediate gp41 immunogen elicits neutralizing antibodies to HIV-1. *J Biol Chem* **289**, 29912-29926 (2014). <https://doi.org:10.1074/jbc.M114.569566>
- 10 Huang, J. *et al.* Broad and potent neutralization of HIV-1 by a gp41-specific human antibody. *Nature* **491**, 406-412 (2012). <https://doi.org:10.1038/nature11544>
- 11 Krebs, S. J. *et al.* Longitudinal Analysis Reveals Early Development of Three MPER-Directed Neutralizing Antibody Lineages from an HIV-1-Infected Individual. *Immunity* **50**, 677-+ (2019). <https://doi.org:10.1016/j.immuni.2019.02.008>
- 12 Haddox, H. K., Dingens, A. S. & Bloom, J. D. Experimental Estimation of the Effects of All Amino-Acid Mutations to HIV's Envelope Protein on Viral Replication in Cell Culture. *PLoS pathogens* **12**, e1006114 (2016). <https://doi.org:10.1371/journal.ppat.1006114>
- 13 Vranken, W. F., Budesinsky, M., Fant, F., Boulez, K. & Borremans, F. A. M. The complete Consensus V3 loop peptide of the envelope protein gp120 of HIV-1 shows pronounced helical character in solution. *FEBS Letters* **374**, 117-121 (1995). [https://doi.org:10.1016/0014-5793\(95\)01086-t](https://doi.org:10.1016/0014-5793(95)01086-t)
- 14 Catasti, P., Fontenot, J. D., Bradbury, E. M. & Gupta, G. Local and Global Structural Properties of the HIV-MN V3 Loop. *Journal of Biological Chemistry* **270**, 2224-2232 (1995). <https://doi.org:10.1074/jbc.270.5.2224>
- 15 Shaik, M. M. *et al.* Structural basis of coreceptor recognition by HIV-1 envelope spike. *Nature* **565**, 318-323 (2019). <https://doi.org:10.1038/s41586-018-0804-9>
- 16 Pan, R. *et al.* Increased Epitope Complexity Correlated with Antibody Affinity Maturation and a Novel Binding Mode Revealed by Structures of Rabbit Antibodies against the Third Variable Loop (V3) of HIV-1 gp120. *J Virol* **92** (2018). <https://doi.org:10.1128/JVI.01894-17>
- 17 Burke, V. *et al.* Structural basis of the cross-reactivity of genetically related human anti-HIV-1 mAbs: implications for design of V3-based immunogens. *Structure* **17**, 1538-1546 (2009). <https://doi.org:10.1016/j.str.2009.09.012>
- 18 Stephenson, K. E. *et al.* Quantification of the epitope diversity of HIV-1-specific binding antibodies by peptide microarrays for global HIV-1 vaccine development. *J Immunol Methods* **416**, 105-123 (2015). <https://doi.org:10.1016/j.jim.2014.11.006>

- 19 Jiang, X. *et al.* Conserved structural elements in the V3 crown of HIV-1 gp120. *Nature structural & molecular biology* **17**, 955-961 (2010). <https://doi.org:10.1038/nsmb.1861>
- 20 Stanfield, R. L., Gorny, M. K., Zolla-Pazner, S. & Wilson, I. A. Crystal Structures of Human Immunodeficiency Virus Type 1 (HIV-1) Neutralizing Antibody 2219 in Complex with Three Different V3 Peptides Reveal a New Binding Mode for HIV-1 Cross-Reactivity. *Journal of Virology* **80**, 6093-6105 (2006). <https://doi.org:10.1128/jvi.00205-06>
- 21 Han, Q. *et al.* Difficult-to-neutralize global HIV-1 isolates are neutralized by antibodies targeting open envelope conformations. *Nature Communications* **10** (2019). <https://doi.org:10.1038/s41467-019-10899-2>
- 22 Lu, M. *et al.* Associating HIV-1 envelope glycoprotein structures with states on the virus observed by smFRET. *Nature* **568**, 415-419 (2019). <https://doi.org:10.1038/s41586-019-1101-y>
- 23 Munro, J. B. *et al.* Conformational dynamics of single HIV-1 envelope trimers on the surface of native virions. *Science (New York, N.Y.)* **346**, 759-763 (2014). <https://doi.org:10.1126/science.1254426>
- 24 Ruprecht, C. R. *et al.* MPER-specific antibodies induce gp120 shedding and irreversibly neutralize HIV-1. *J Exp Med* **208**, 439-454 (2011). <https://doi.org:10.1084/jem.20101907>
- 25 Walser, M. *et al.* *Highly potent anti-SARS-CoV-2 multi-DARPin therapeutic candidates* (Cold Spring Harbor Laboratory, 2020).